



# A partially coupled hydro-mechanical analysis of the Bengal Aquifer System under hydrological loading

Nicholas D. Woodman<sup>1,a</sup>, William G. Burgess<sup>1</sup>, Kazi Matin Ahmed<sup>2</sup>, and Anwar Zahid<sup>3</sup>

<sup>1</sup>Department of Earth Sciences, University College London, London WC1E 6BT, UK

<sup>2</sup>Department of Geology, Dhaka University, Dhaka 1000, Bangladesh

<sup>3</sup>Bangladesh Water Development Board, Dhaka, Bangladesh

<sup>a</sup>current address: Faculty of Engineering and the Environment, University of Southampton, Southampton SO17 1BJ, UK

**Correspondence:** Nicholas D. Woodman (n.d.woodman@soton.ac.uk)

Received: 4 June 2018 – Discussion started: 25 July 2018

Revised: 22 March 2019 – Accepted: 8 April 2019 – Published: 22 May 2019

**Abstract.** The coupled poro-mechanical behaviour of geologic-fluid systems is fundamental to numerous processes in structural geology, seismology, and geotechnics, but is frequently overlooked in hydrogeology. Substantial poro-mechanical influences on groundwater head have recently been highlighted in the Bengal Aquifer System, however, driven by terrestrial water loading across the Ganges–Brahmaputra–Meghna floodplains. Groundwater management in this strategically important fluvio-deltaic aquifer, the largest in southern Asia, requires a coupled hydro-mechanical approach which acknowledges poroelasticity. We present a simple partially coupled, 1-D poroelastic model of the Bengal Aquifer System, and explore the poro-mechanical responses of the aquifer to surface boundary conditions representing hydraulic head and mechanical load under three modes of terrestrial water variation. The characteristic responses, shown as amplitude and phase of hydraulic head in depth profile and of ground surface deflection, demonstrate (i) the limits to using water levels in piezometers to indicate groundwater recharge, as conventionally applied in groundwater resources management; (ii) the conditions under which piezometer water levels respond primarily to changes in the mass of terrestrial water storage, as applied in geological weighing lysimetry; (iii) the relationship of ground surface vertical deflection with changes in groundwater storage; and (iv) errors of attribution that could result from ignoring the poroelastic behaviour of the aquifer. These concepts are illustrated through application of the partially coupled model to interpret multi-level piezometer data at two sites in southern Bangladesh. There is a need for further re-

search into the coupled responses of the aquifer due to more complex forms of surface loading, particularly from rivers.

## 1 Introduction

Throughout the Bengal Basin, the floodplains of the Ganges, Brahmaputra, and Meghna (GBM) rivers (Fig. 1) are underlain by the Bengal Aquifer System (BAS), the largest aquifer in southern Asia and the source of water to over 100 million people (Burgess et al., 2010). More than 10 million tubewells throughout the basin provide water from the BAS for domestic use and for irrigation of the rice crop (Ravenscroft et al., 2009); these include hand-pumped tubewells, normally between 15 and 30 m depth below ground level (b.g.l.), for domestic use, and tubewells installed with motor-driven pumps to abstract water from between 50 and 75 m depth b.g.l. for irrigation of the dry season rice crop (January to April). Municipal water supplies commonly abstract year-round from depths between 200 and 300 m b.g.l. (Shamsudduha et al., 2018). Management of the BAS groundwater resource relies on monitoring water levels in networks of observation boreholes, taking the conventional approach that changes in groundwater heads represent volumetric changes in groundwater storage through recharge and drainage (Shamsudduha et al., 2011). This approach presumes the hydraulic behaviour of the aquifer to be decoupled from its mechanical response to changes in stress. Recently, however, the distinctively poroelastic behaviour of the BAS has been recognized (Burgess et al., 2017), by which groundwater heads are sub-

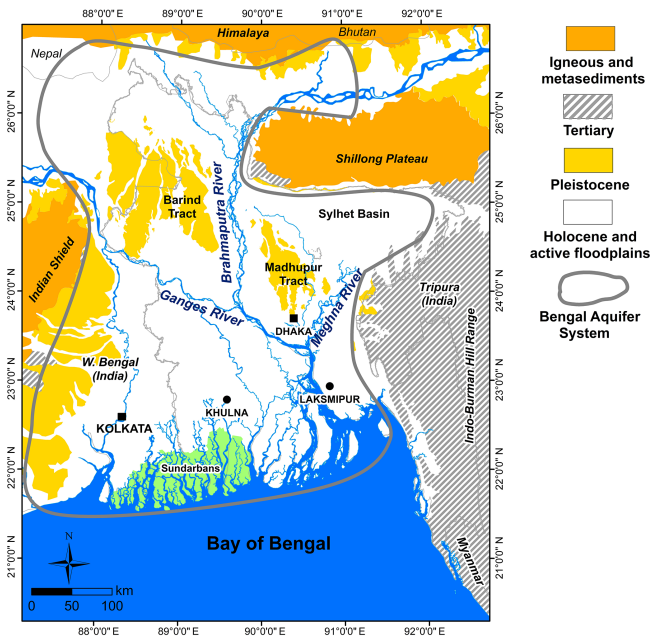


**Figure 1.** Location map showing the extent of the Bengal Aquifer System (BAS) and the Ganges–Brahmaputra–Meghna (GBM) floodplains.

ject to substantial mechanical perturbation driven by changes in the mass of terrestrial water storage (TWS) above the surface of the aquifer. A coupled hydro-mechanical approach is necessary for understanding groundwater conditions and managing resources in this environment, particularly in relation to recharge (Shamsudduha et al., 2012), sustainability of groundwater abstraction for irrigation (Shamsudduha et al., 2011) and municipal water supply (Ravenscroft et al., 2013), and the security of schemes for mitigation against groundwater arsenic (Michael and Voss, 2008) and salinity (Rahman et al., 2011; Sultana et al., 2015).

The generally coupled poro-mechanical nature of geologic-fluid systems is well-established (Neuzil, 2003); porewater pressures affect the stress state and vice versa. These interactions are accepted as important where groundwater conditions are related to faulting (Roeloffs, 1988; Rojstaczer and Agnew, 1989; Sutherland et al., 2017), earthquakes (Manga et al., 2012), pumping-induced aquitard responses (Verruijt, 1969), ground subsidence (Burbey et al., 2006; Erban et al., 2014), glacial loading effects (Bense and Person, 2008; Black and Barker, 2016), and surface water interactions (Acworth et al., 2015; Boutt, 2010). Use of ground surface vertical displacements to infer aquifer or groundwater conditions (Chaussard et al., 2014; Reeves et al., 2014) is also predicated on coupling of the hydraulic and mechanical behaviour of aquifer sediments. For simulation of transient groundwater flow in aquifers, however, a decoupling simplification is frequently applied such that the elastic equation does not need to be solved simultaneously.

Thus, the flow equation is solved without consideration of internal stresses and strains or mechanical boundary conditions. Despite this, the poro-mechanical nature of confined aquifers is embedded in the concept of specific storage which incorporates the elastic compressibility of the aquifer materials (Domenico and Schwartz, 1998; Green and Wang, 1990; Narasimhan, 2006). Furthermore, it is associated with the well-known concept of barometric efficiency (Spaine, 2002), which describes the response of groundwater pressure to variations in atmospheric pressure, perhaps the example of surface loading effects most familiar to hydrogeologists. The decoupling assumption is reasonable where the effects of mechanical loading can be considered insignificant, either when the changes in load are small or when the applied load is mostly borne by the solid rather than the fluid (Black and Barker, 2016). Neither of these conditions apply to the BAS sediments, which are highly compressible (Steckler et al., 2010) and subject to substantial and extensive TWS mechanical loads due to heavy rainfall, deep flooding, and large river discharges as a consequence of the annual monsoon (Shamsudduha et al., 2012).

In the event of laterally extensive changes to mechanical loads and/or hydraulic heads above the surface of an aquifer, and laterally homogeneous aquifer properties, by symmetry it may be deduced that lateral strains are zero. This condition gives rise to a *partial* coupling of the elastic and fluid pressure equations (Neuzil, 2003). In the case of *partial* coupling, changes to the mechanical load due to the changing mass of water near or at the surface may be included within the flow equation, one-dimensionally in the vertical direction, and the solutions will satisfy all the equilibrium and compatibility requirements for stress and strain. There is no need to solve the elastic equation in order to calculate pressures in the aquifer, although once the flow equation is solved, the pressures can be substituted into the elastic equation to provide stresses and strains (Anochikwa et al., 2012). A sub-set of this partially coupled condition occurs where there is negligible groundwater flow, due to very low hydraulic gradients, low permeability, or a combination of both. This can be the situation in extensive fluvio-deltaic aquifers of low topographic relief such as the BAS (Burgess et al., 2017) if mechanical loading is imposed at the surface in a manner which does not induce significant vertical hydraulic gradients. Under these conditions, porewater pressures are determined by changes to surface mechanical loading alone, and changes in groundwater head may be taken as a measure of changes in TWS mechanical loading above the surface of the aquifer. This is the conceptual basis for geological weighing lysimetry (van der Kamp and Schmidt, 1997, 2017; Bardsley and Campbell, 1994, 2007) as used in diverse environments to determine  $\Delta$ TWS at the scale of individual catchments (Marin et al., 2010; Lambert et al., 2013; Barr et al., 2000; Smith et al., 2017). Geological weighing lysimetry has been suggested as suitable for mapping the variability of  $\Delta$ TWS within the Bengal Basin (Burgess et al., 2017; Bardsley and Campbell,

2000), complementary to basin-scale estimates based on the Gravity and Climate Recovery Experiment (GRACE) satellite mission (Tapley et al., 2004; Tiwari et al., 2009; Sham-sudduha et al., 2012).

The purpose of this paper is to explore the behaviour of the BAS as a poroelastic aquifer subject to a variety of extensive TWS mechanical and hydraulic loads. Poro-elastic theory is very well-established, but has not previously been applied in the context of a thick and extensive aquifer such as the BAS to show the implications for groundwater pressures together with solid strains and ground surface displacements.

The Bengal Basin has a tropical climate dominated by the Indian monsoon, with annual rainfall increasing from 1500 mm in the south and west to 5500 mm in north-eastern Bangladesh, of which 85 % falls during the summer rainy season (May to November) when individual storm events can contribute over 100 mm d<sup>-1</sup> (Ravenscroft, 2003). During the monsoon season, river levels rise by 2–8 m, leading to widespread flooding (Steckler et al., 2010), with up to 30 % of the land surface routinely being flooded to a depth of up to ca. 1 m. During the Boro rice irrigation season (January to April), groundwater pumping for irrigation throughout rural areas commonly provides standing water across rice paddies to a depth of ca. 0.1 m (Hasanuzzaman, 2003). For the purpose of this paper, we treat the separate components of TWS across the GBM floodplains as *inundation* (free-standing surface water such as paddy, floods, beels, and ponds), *unconfined storage* (water in the unsaturated zone and in saturated pores in the intermittently saturated zone of the aquifer), *elastic storage* (water in the saturated pores in the permanently saturated zone), and *rivers* (surface water flowing in rivers and drainage channels). Processes that alter the TWS loads include rainfall and evaporation, rising and falling river stage, flooding and drainage of the land surface, varying soil moisture storage, and a fluctuating water table. Groundwater pumping modifies the water balance and induces additional hydro-mechanical responses. These processes differ in their timing, the geometry of the TWS stores they affect, and the relationship between their resultant hydraulic and mechanical expressions. First, we apply the concept of *partial* coupling to seek characteristic responses of the aquifer to extensive TWS loads originating as (a) surface water inundation, (b) water table fluctuation, and (c) water bodies hydraulically isolated from the aquifer. These loading styles are examined with and without pumping. The results address important questions for the BAS which are likely also relevant to similarly extensive and strategically important fluvio-deltaic aquifer systems elsewhere in southern Asia (Fendorf et al., 2010; Benner et al., 2008; Larsen et al., 2008; Tam et al., 2014; Xu et al., 2011): how can piezometer heads in the poroelastic aquifer be used to indicate recharge, as required for conventional groundwater resources management; under what conditions can piezometer heads be used to measure  $\Delta$ TWS using geological weighing lysometry; can ground surface deflections be related to changes in groundwater stor-

age; and what errors may arise if the poroelastic behaviour of the aquifer is ignored? Second, we apply the partial-coupling approach to these questions in the BAS, with reference to multi-level piezometer data from Khulna and Laksmipur in southern Bangladesh (Fig. 1).

## 2 Methods

We firstly set out the partially coupled 1-D poro-mechanical approach that we use to examine the implications of specific surface (upper boundary) loading scenarios, with aquifer parameters set to represent the BAS underlying the GBM floodplains (Fig. 1). We consider an equivalent homogeneous uniform medium, as well as a layered structure based on lithological sections. The results provide a diagnostic framework which we apply to analysis of loading styles at Khulna and Laksmipur in southern Bangladesh.

### 2.1 Poro-mechanical equations

We concentrate on the coupling between water flow and the mechanical behaviour of the BAS sediment, assuming isothermal conditions and that the aquifer material behaves in a linear-elastic way. This is likely to be reasonable under repeated mechanical load–unload cycles, provided there is no secular decline in groundwater level sufficient to cause effective stress to exceed the previous loading maximum.

The 3-D flow and mechanical equations are given in the Appendix. In the event of uniform (1-D) areal mechanical loading, and where lateral strains are negligible, the system simplifies to a flow equation coupled to a mechanical equation for 1-D loading:

$$\nabla \cdot \kappa (\nabla p + \rho g \nabla z) = S_s \frac{\partial p}{\partial t} - S_s \xi \frac{\partial \sigma_{zz}}{\partial t} - g J, \quad (1)$$

where  $\kappa$  is the hydraulic conductivity (m s<sup>-1</sup>),  $\rho$  is the fluid density (kg m<sup>-3</sup>),  $p$  is the pore pressure (Pa),  $z$  is the elevation (m),  $J$  (kg m<sup>-3</sup> d<sup>-1</sup>) is a fluid source term used here to simulate groundwater abstraction by pumping,  $\xi$  is the 1-D loading efficiency (given in Appendix Eq. A5),  $\nu$  is Poisson's ratio (–), and  $S_s$  is the 1-D specific storage typically used in groundwater analyses (van der Kamp and Gale, 1983).

The sediment is assumed to sit on a rigid base, with the top surface free to move, so strain can only be vertical. Thus from Eq. (A1), the vertical stress and strains are related by

$$\sigma_{zz} = K' \varepsilon_{zz} + \alpha_B p, \quad (2)$$

where  $K' = 3K(1 - \nu)/(1 + \nu)$ ,  $\alpha_B$  is the Biot–Willis coefficient (assumed equal to 1 to simulate incompressible particle grains), and the bulk modulus,  $K$ , and shear modulus,  $G$ , are related to Young's modulus  $E$  by  $K = \frac{E}{3(1-2\nu)}$  and  $G = \frac{E}{2(1+\nu)}$ . Changes to the total vertical stress,  $\sigma_{zz}$  (here termed “mechanical loads”), are applied as a boundary condition at the surface, and are transmitted by the solid skele-

ton to the entire solid at the acoustic velocity. This represents “partial coupling”; if there are negligible internal loads and provided the changes to the surface load are known, then the flow equation (Eq. 1) can be solved without a need to solve the elastic equations. Deformations can be found from Eq. (2), in conjunction with the compatibility relationships.

The simplified system considered here is given in Fig. 2. On the upper boundary, the changing TWS is simulated by means of a changing head and a changing mechanical load, according to the nature of the contributing hydrological components. Under this simplification, vertical displacement at the surface will arise in only two ways: by contraction or expansion of the pore space where there is a net change in the volume of water in the column, and by contraction or expansion of the porewater. Being limited to 1-D movement, these volume changes are entirely taken up by vertical displacement.

The reference frame is the base of the model which is assumed fixed in space and set at 1 km depth, acknowledging the variation in aquifer thickness between south-eastern Bangladesh, 3000 m (Michael and Voss, 2009a), and West Bengal, 300 m (Mukherjee et al., 2007). Within this domain, Eqs. (1) and (2) are solved analytically for a homogeneous uniform material in the absence of pumping, and numerically where layers of individually homogeneous materials are simulated, with and without pumping. Where pumping is simulated, the water is assumed to be taken uniformly from the pumping interval. For simplicity, earth tides are neglected.

## 2.2 Analytical solution

Taking Eq. (1) and assuming homogeneous  $K$  and  $E$  and that  $J = 0$ , converting  $p$  to metres head,  $h$  (i.e.  $h = \rho g p + z$ ), and  $\sigma_{zz}$  to metres of load (i.e.  $L = \sigma_t / \rho g$  where  $\rho$  ( $\text{kg m}^{-3}$ ) is the density of water and  $g$  ( $\text{m s}^{-2}$ ) is the acceleration due to gravity) (Anochikwa et al., 2012; van der Kamp and Schmidt, 1997) gives

$$D \frac{\partial^2 h}{\partial z^2} = \frac{\partial h}{\partial t} - \xi \frac{\partial L}{\partial t}, \quad (3)$$

where 1-D hydraulic diffusivity is defined as  $D = \frac{\kappa}{S_s}$ .

We apply the following sinusoidal hydraulic and mechanical loading boundary conditions to Eq. (9), where we introduce a parameter,  $\alpha$ , which can be set to zero to give the case of a load in the absence of a varying head, and which otherwise is kept at 1:

$$\begin{aligned} h(0, t) &= H(t) = \alpha H_0 \cos(\omega t), \\ L(t) &= S_y H_0 \cos(\omega t). \end{aligned} \quad (4)$$

The following solution is obtained:

$$h(z, t) = \alpha B \cos(\omega t - \psi), \quad (5)$$

where  $\psi$  is the lag (in radians) behind the head  $H(t)$  and mechanical loads  $L(t)$  at the boundary and

$$B = \sqrt{\gamma^2 + 2\gamma(\alpha - \gamma)e^{-\theta} \cos(\theta) + (\alpha - \gamma)^2 e^{-2\theta}}, \quad (6)$$

$$\psi = \tan^{-1} \left( \frac{(\alpha - \gamma) \sin(\theta)}{(\alpha - \gamma) \cos(\theta) + \gamma e^{\theta}} \right),$$

$$\theta = z \sqrt{\frac{\omega}{2D}} = z \sqrt{\frac{\pi}{DT}} \quad \text{and} \quad \gamma = S_y \xi.$$

In the event that the mechanical load,  $L$ , is negligible compared to applied head  $H$  (e.g. where either  $S_y$  is very small or  $\xi$  is very small), the hydraulic-only solution is well-known (van der Kamp and Maathuis, 1991):

$$h(z, t) = H_0 \exp(-\psi) \cos(\omega t - \psi), \quad (7)$$

where the lag is now  $\psi = \theta$ . Thus, the lag increases with depth or with increasing forcing frequency and the amplitude decreases exponentially with  $\theta$ .

Displacement and change in groundwater storage can be calculated as the time integral of velocity at the surface. Applying Darcy’s law at the surface ( $z = 0$ ) and integrating gives

$$u = \Delta S = \int_0^t \kappa \left. \frac{dh}{dz} \right|_{z=0} dt'. \quad (8)$$

Equation (8) can be computed by differentiating Eq. (5) with respect to  $z$  and then numerically integrating over time. Alternatively, the change in storage can be reported from the numerical model.

## 2.3 Numerical solution

We used the COMSOL Multiphysics<sup>®</sup> software (COMSOL Multiphysics<sup>®</sup>, 2018), validated against the analytical solutions for uniform permeability, to solve the stress and flow Eqs. (1) and (2). The finite-element model is unrestricted in terms of spatial distribution of parameter properties and in terms of the boundary condition functions.

## 2.4 Parameter allocation

Selected parameter values for the BAS underlying the GBM floodplains are given in Fig. 2. The bulk values for the uniform representations are close to the harmonic average of the series components. We next discuss the context in which these parameter selections are made.

### 2.4.1 Modulus of elasticity, storativity, and loading efficiency

Textbook  $S_s$  values (Domenico and Schwartz, 1998) for the materials in the Bengal Basin range between approximately  $1 \times 10^{-5} \text{ m}^{-1}$  (dense sandy gravel) and  $1 \times 10^{-2} \text{ m}^{-1}$  (plastic clay). In large-scale modelling of head recession data in

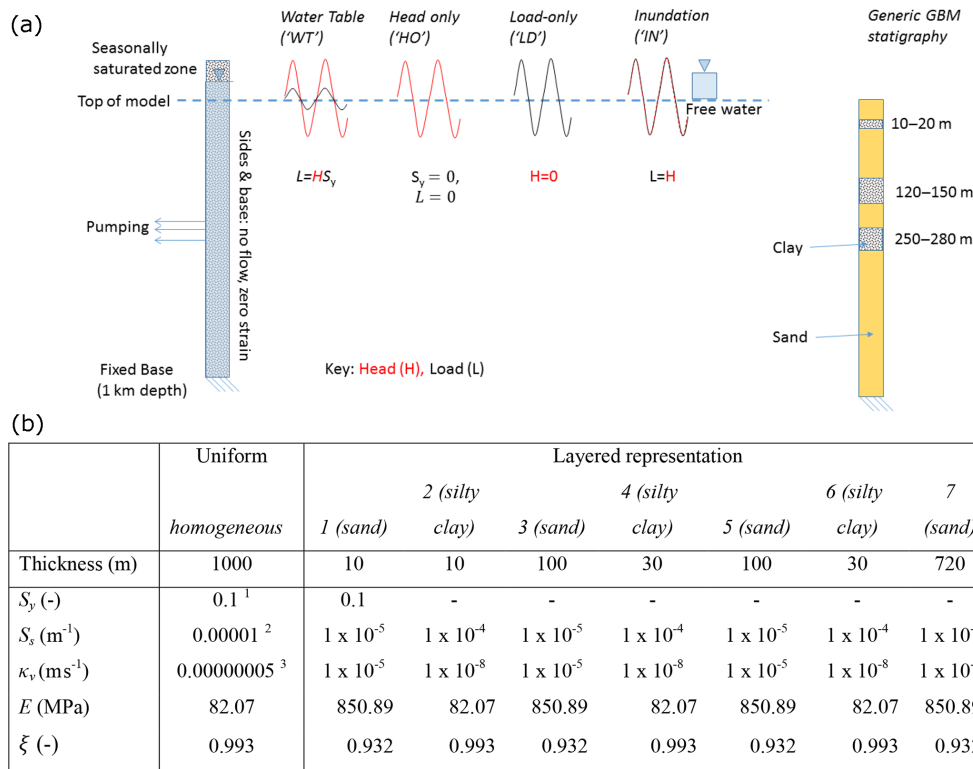


**Figure 2.** The 1-D model showing (a) the upper surface boundary conditions with head as red lines and mechanical load (weight) as black lines, expressed as metres of water, and a representative stratigraphy for the BAS underlying the GBM floodplains, with the profile depth being 1 km; and (b) parameter values for the uniform and layered 1-D representations. Porosity is taken as 0.1 throughout;  $\nu = 0.25$ ;  $E$  and  $\xi$  are calculated using Eqs. (A3), (A4), and (A5). <sup>1</sup> Shamsudduha et al. (2011); <sup>2</sup> Burgess et al. (2017); <sup>3</sup> Michael and Voss (2009a).

the basin Michael and Voss (2009b) achieved their best fits when  $S_s$  was  $9.4 \times 10^{-5} \text{ m}^{-1}$ , taking pumped abstraction to be areally uniform. This is the basis for the range in specific storage,  $S_s$ , for the BAS (Fig. 2).

Specific storage  $S_s$  and Young’s modulus  $E$  are related though Eq. (A3) and to the loading efficiency  $\xi$  via Eq. (A4). These inter-relationships are plotted in Fig. 3. It is notable that for  $E < 1 \text{ GPa}$ ,  $\xi > 0.95$  and  $S_s > 1 \times 10^{-5} \text{ m}^{-1}$ . Thus the loading efficiency only falls significantly below 1 for materials stiffer than around 1 GPa, and where the specific storage is less than  $1 \times 10^{-5} \text{ m}^{-1}$ . Uncemented sediment is thus expected to have  $\xi \sim 1$  (Bakker, 2016); on this basis the BAS sediment is unlikely to be sufficiently stiff in the top few hundred metres to allow decoupling of the stress and flow equations. This is corroborated by in situ, high-pressure dilatometer measurements (de Silva et al., 2010) giving  $E$  within the broad range for sediments given in Fig. 3.

Estimates of (1-D) loading efficiency based (Jacob, 1940) on barometric efficiency are rather lower: a range of 0.69–0.87 has been determined at Laksmipur in the GBM sediment (Burgess et al., 2017). This is potentially indicative of a considerable stiffening due to burial ( $E$  in the range 6–17 GPa), indicating  $S_s$  in the range  $1 \times 10^{-6}$  to  $9 \times 10^{-8} \text{ m}^{-1}$ . Such a condition might be expected in a Gibson soil (Gib-

son, 1974; Powrie, 2014). However, the Laksmipur estimates do not decrease systematically with depth, possibly due to changes in stiffness in different materials. The discrepancy may alternatively be related to the timescale of processes responsible for changes in groundwater pressure. Barometric efficiency measurements operationally consider short-term pore pressure changes likely corresponding to the response of relatively stiff aquifer sands, whereas pressure changes in clays are expected to become significant in the longer term. Where short-term moisture loading effects are the key interest (Anochikwa et al., 2012; Bardsley and Campbell, 2000), values for loading efficiency derived from barometric efficiency may be the most appropriate. Here however our main concern is for poro-mechanical consistency and for water load changes operating over a range of timescales; therefore, we adopt  $S_s$  estimates based on aquifer pumping tests and use the corresponding  $\xi$  and  $E$  values (Fig. 3).

### 2.4.2 Hydraulic conductivity

Basin-scale modelling suggests a horizontal–vertical anisotropy for hydraulic conductivity in the BAS of  $\sim 10000$  (Michael and Voss, 2009b; Ravenscroft et al., 2005). This may be explained as an effective, large-scale

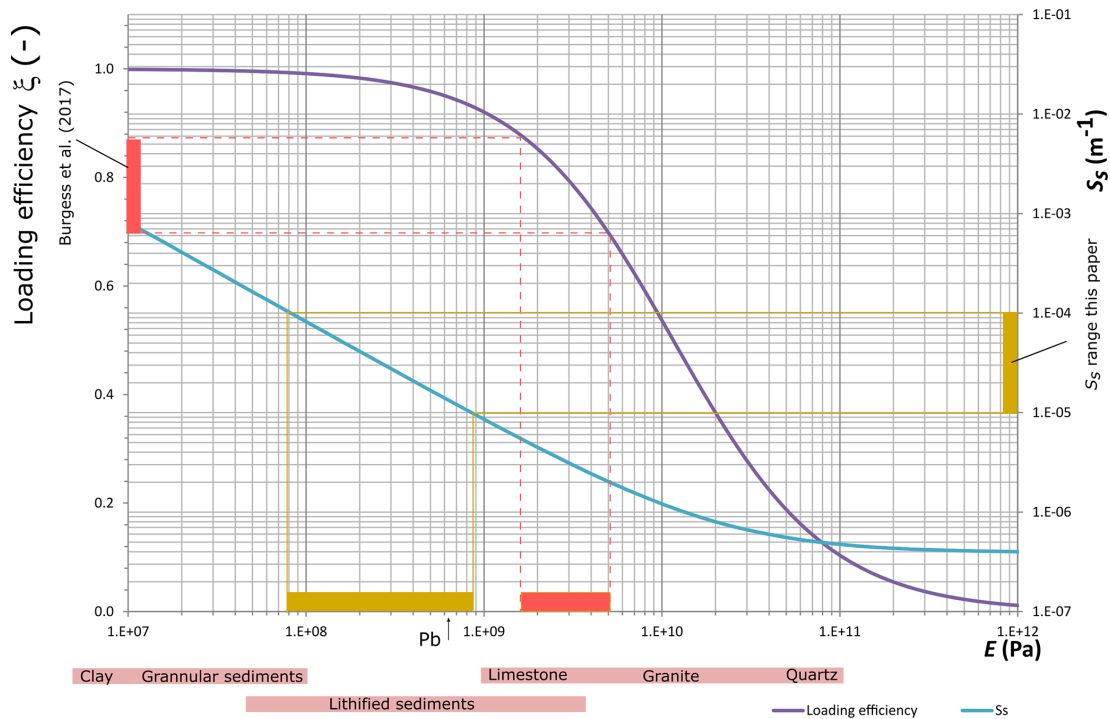


**Figure 3.** Relationship between 1-D specific storage ( $S_s$ ), Young's modulus ( $E$ ), and 1-D loading efficiency ( $\xi$ ) using Eqs. (A3), (A4), and (A5) assuming a porosity of 0.1 and Poisson's ratio of 0.25. Projections show the corresponding inferred ranges of  $E$  based on the  $S_s$  range applied ( $1 \times 10^{-5}$ – $1 \times 10^{-4} \text{ m}^{-1}$ ) and the loading efficiencies calculated via barometric efficiency estimates (0.69–0.87) by Burgess et al. (2017). Pink bars show indicative ranges for common geological materials. Arrow indicates data from 73 m depth at Padma Bridge (Pb) (de Silva et al., 2010).

value incorporating finer-scale detail of the highly heterogeneous sedimentary record of the past deltaic environment where low-permeability lenses and drapes are laterally discontinuous (Hoque et al., 2017). Michael and Voss (2009a) cite aquifer tests (Hussain and Abdullah, 2001) conducted by the Bangladesh Water Development Board (BWDB) giving a range for hydraulic conductivity ( $\kappa$ ) from  $3 \times 10^{-5}$  to  $1 \times 10^{-3} \text{ m s}^{-1}$ . Accounting for anisotropy,  $\kappa_v$  may therefore locally be in the range  $\sim 1 \times 10^{-9}$  to  $1 \times 10^{-7} \text{ m s}^{-1}$ . The  $\kappa_v$  values of the uniform and layered representations of the BAS underlying the GBM floodplains (Fig. 2) and of silty clay in layered representations of the Khulna and Laksmipur sites (Sect. 4) lie within this range.

### 2.4.3 Specific yield

Specific yield is the drainable porosity of the material in which the water table moves. Michael and Voss (2009b) cite a range from 0.02 to 0.19 in Bangladesh, noting that much of the basin has a specific yield in the range of 0.02–0.05. We take  $S_y = 0.1$  and 0.01 as order-of-magnitude values typical of sand and clay respectively (Domenico and Schwartz, 1998).

## 2.5 Upper boundary conditions and groundwater abstraction

Changes to the shallow water budget which have the potential to be laterally extensive and uniform include water arriving as rainfall at the surface and either ponding or moving to the shallow water table as recharge; and water departing the surface or the water table by evaporation, or as runoff to the extensive network of drainage channels. Pumping for domestic and irrigation supply may potentially be considered areally uniform, where sufficiently common and over a wide area (Michael and Voss, 2008). The changing shallow water budget causes a change in mechanical loading to the aquifer system, and if in direct hydraulic continuity with the saturated water column it also causes a change in head. If the shallow water is not hydraulically connected to the saturated aquifer system, the effects of the changing water budget are transmitted to depth by mechanical compression/extension of the sediment, but not by hydraulic diffusion. Changes to the barometric pressure also apply a laterally extensive changing force to the surface of the aquifer and to the water column, and earth tides are also laterally extensive. The daily perturbation on water heads by atmospheric pressure changes is of the order of 0.01 m (Burgess et al., 2017), which is small compared to the annual hydrograph amplitude of the order of

1 m. Barometric pressure and earth tides are both neglected for simplicity here.

To explore the consequences of these hydraulic and mechanical loading sources, the groundwater dynamics associated with three upper surface boundary conditions are modelled here (Fig. 2). Firstly, the effect of a changing level of free water is examined, such as would be seen in paddy fields, ponds, or during floodwater inundation. This condition is here termed “IN”. The change in free-water level is equal to both the change in head and the change in mechanical load at the upper surface (load is here parameterized in metres of water rather than as a stress). Secondly, the effect of changes to unconfined storage due to a moving water table is examined. This condition is here termed “WT”. The change in load is the specific yield times the head. For very small specific yields this condition approaches the hydraulic-only (“HO”) loading case, whereby there is insignificant mechanical load despite the change in head. Thirdly, we examine the effect of a changing surface water store (which could be either free water held above an impermeable barrier, or a perched phreatic aquifer) which is hydraulically isolated from the main aquifer system. A mechanical load only is applied; therefore, no head change is applied to the aquifer, and this condition is termed “LD”.

These three TWS loading scenarios are applied in turn to a uniform and layered representation of the BAS underlying the GBM floodplains. The loading is applied as sinusoidal functions with unit amplitude and a time period of 1 year to simulate the annual hydrological cycle. Additionally, the effects of groundwater abstraction are simulated. Abstraction is taken evenly from the depth interval 50–100 m at an average rate of  $0.2 \text{ m a}^{-1}$ , either as continuous pumping or as discontinuous pumping  $\pi$  out of phase with the TWS load, as a coarse representation of seasonally varying pumping for irrigation during the dry season.

### 3 Forward modelling results

The modelled responses of groundwater head to sinusoidal hydraulic and mechanical source terms, together with changes in groundwater storage and ground surface vertical displacements, are illustrated for the GBM environment with uniform properties in Figs. 4 and 5. Figure 4 shows the modelled responses over 10 years at depths of 30, 100, and 300 m, approximating typical BWDB multi-level piezometers (BWDB, 2013). The depth variations of amplitude and phase for groundwater head and the phase lag for surface displacement are summarized in Fig. 5. The effect of layering (Supplement) is to cause departure from the uniform cases, so interpretation of data in a real, heterogeneous aquifer should take into account local deviation from idealized uniform conditions. However, in general, the loading style (“IN”, “WT”, “LD”) and pumping regime are of

more significance for the head responses and surface displacements than the detail of the BAS stratigraphy.

#### 3.1 The free-surface water inundation scenario (“IN”)

Under free-surface water inundation, head changes are characteristically equal in amplitude at all depths and in phase with the inundation signal. Away from the top boundary, the instantaneous head due to loading in this case is  $h = \xi L$ . Since  $\xi$  is close to 1 and  $H = L$ , the head is everywhere almost equal to the mechanical load given that at the top boundary the head is also  $h = H$ . Therefore, under free-surface water inundation in the absence of pumping, piezometers at all depths can be expected to record the surface water mechanical load, effectively operating as weighing lysimeters. The vertical displacement of the ground surface is extremely small (amplitude  $\sim 0.4 \text{ mm}$ ), being due to the small compression of porewater itself over the 1 km simulated depth, and is out of phase with the load (i.e. the ground surface moves downwards under an increasing load). The amplitude of change in saturated storage is infinitesimal ( $\sim 0.02 \text{ mm}$ ). The system is essentially “un-drained”: water does not flow into or out of the pores, which therefore experience only minimal strain.

#### 3.2 The variable water table scenario (“WT”)

By contrast with the “IN” scenario, head changes determined by a moving water table are depth-variable in amplitude and phase. When  $S_y \rightarrow 0$  the “WT” condition tends to the head-only end-member (“HO”) and when  $S_y \rightarrow 1$  the “WT” condition tends to the “IN” scenario. The maximum lag for  $S_y = 0.1$  is at 137 m depth (or  $\theta = 1.94$ ), beyond which it reduces (Fig. 5b). The sensitivity in head to  $S_y$  for the “WT” scenario is illustrated in Fig. 5c. The amplitude of head responses is less than the water table fluctuation at all depths. Moreover, only a deep piezometer such as the one indicated at 300 m (Fig. 4b) will behave as a weighing lysimeter in this scenario. Here, heads are in phase with the water table and have approximate magnitude,  $h = \xi L = \xi S_y H$ , as in the study by van der Kamp and Maathuis (van der Kamp and Maathuis, 1991) of a thick aquitard overlying a confined aquifer. At 100 m the amplitude of head change is greater than at 300 m and lags behind the water table. At 30 m the amplitude of the head change is greatest and the lag is less than at 100 m. The difference in the head responses compared to the “IN” scenario is due to the difference in magnitudes of the applied head and applied load under the “WT” scenario, causing an instantaneous internal head gradient which subsequently diffuses. Ground surface displacement is  $\sim 4 \text{ mm}$  and lags the load by 44 d. With increased head at the top boundary, the upper surface moves upwards because as higher heads penetrate the aquifer the effective stress is reduced. The lag is due to the time taken for the surface head to diffuse downwards.

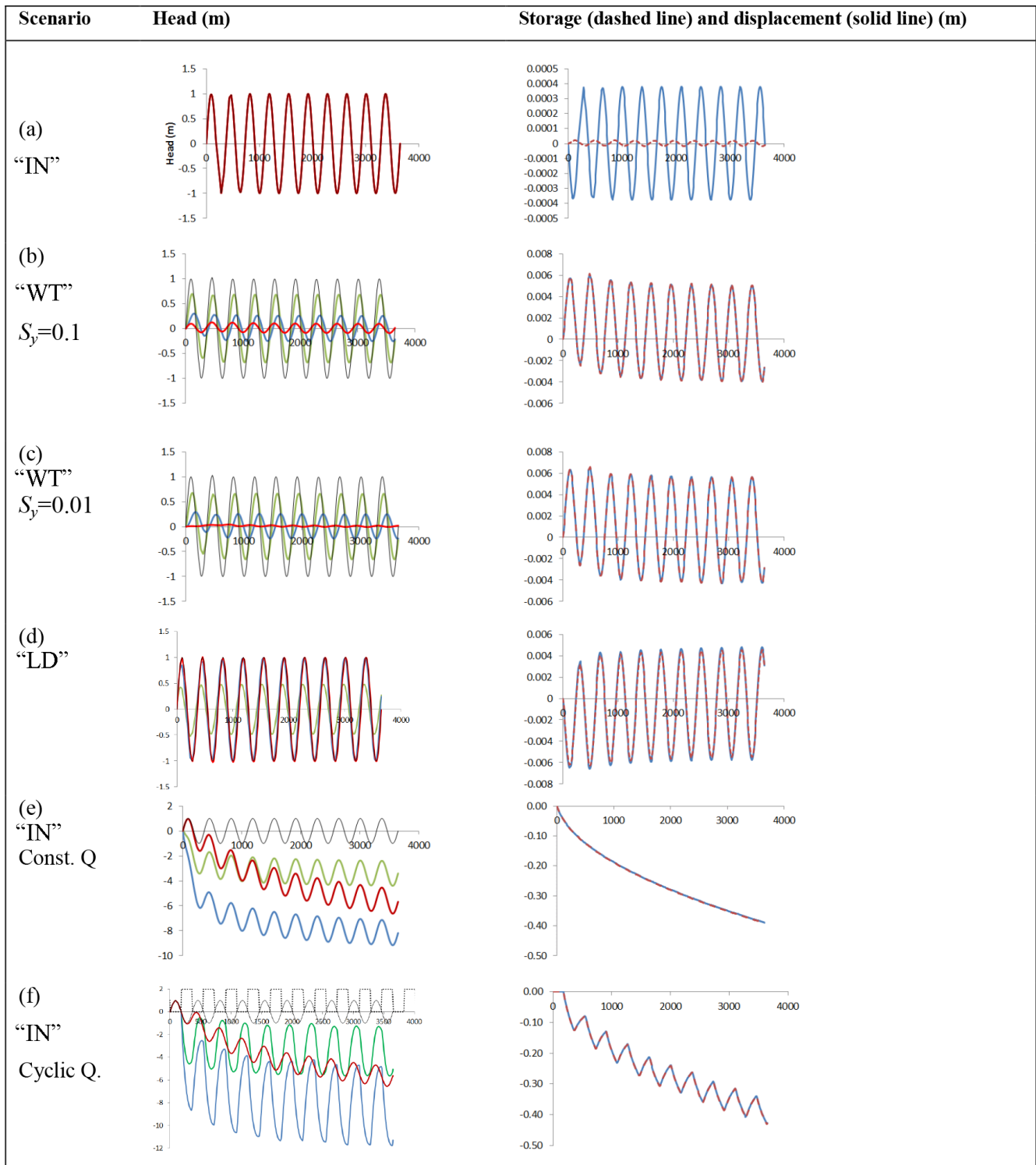


**Figure 4.** 1-D model simulations for the GBM environment, showing results for the scenarios (a) “IN”, (b) “WT” ( $S_y = 0.1$ ), (c) “WT” ( $S_y = 0.01$ ), (d) “LD”, (e) “IN” with constant pumping, and (f) “IN” with cyclic pumping (see text for explanation). The  $x$  axis is time in days, shown to 10 years (i.e. 3650 d). The amplitudes reported in the text are calculated from the max–min of the last annual cycle. Left: the  $y$  axis is head, in metres (m). The surface head and/or mechanical load boundary conditions (black line) are expressed as equivalent metre head (for the WT condition the unit variation of head is given and the  $S_y$  variation in mechanical load is not shown); results are in green (30 m depth), blue (100 m depth), and red (300 m depth) in all cases. For panel (a) results are co-linear at all depths; for panel (f) the intermittent pumping is shown as off/on by the square-wave dotted line. Right: the  $y$  axis has dimension of length, in metres (m), showing changes in storage (dashed red line) and surface displacement (solid blue line) for each scenario.



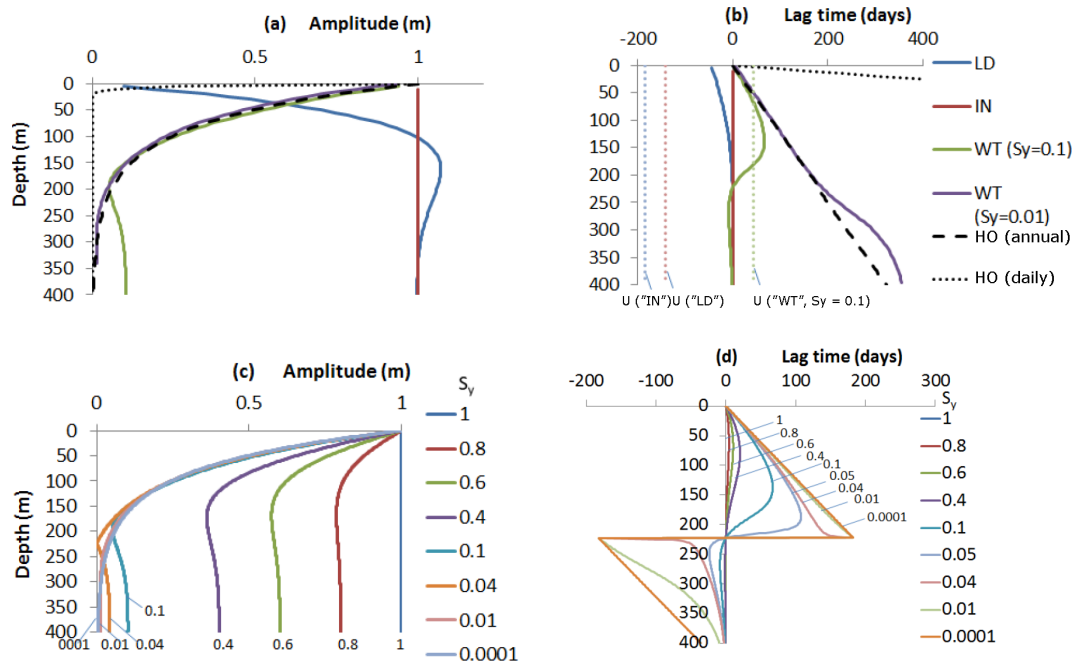


**Figure 5.** Profiles with depth for (a) amplitude of head response, (b) phase of head response and surface displacement ( $U$ ), (c) sensitivity of amplitude to  $S_y$  for the “WT” boundary condition, and (d) sensitivity of phase to  $S_y$  for the “WT” boundary condition. For panels (a) and (b), the colour code for scenarios “LD”, “IN”, “WT” ( $S_y = 0.1$ ), “WT” ( $S_y = 0.01$ ), and HO is shown in panel (b) (see text for explanation); in panel (b), displacement for the WT,  $S_y = 0.01$ , scenario overlies that for the WT,  $S_y = 0.1$  scenario, and so is not shown. (Note: in the instance that  $\xi$  is not close to 1,  $S_y$  in these plots can be substituted by  $\gamma = S_y \xi$ .)

### 3.3 The hydraulically disconnected load scenario (“LD”)

Heads in the case of a surface load hydraulically isolated from the aquifer show a third characteristic behaviour. In this case the amplitude of head change increases from zero at the top boundary (Fig. 5a), reaching a peak which is greater than the load, 1.07 at 162 m (or  $\theta = 2.29$ ). The amplitude thereafter tends to  $\xi L$  at greater depth, whilst the lag tends to zero. Therefore heads in relatively deep piezometers potentially represent the surface load under a “LD” boundary condition, as in Fig. 4d, where the heads at 300 m match the surface load, whereas at 30 m they do not. This is due to upward head diffusion towards the surface where the head boundary condition is  $h = 0$ . The lag which occurs in the “WT” scenario due to the applied head exceeding the mechanical load is reversed in this “LD” scenario, becoming a lead time as the applied load exceeds the applied head. Surface displacement is out of phase with the load, leading by  $\sim \pi$  radians. The ground surface displacement amplitude of  $\sim 4$  mm is 10 times greater than for the “IN” scenario, but is still very small in comparison to the annual variability of order 10 cm measured by GPS (Steckler et al., 2010). The “LD” behaviour can be interpreted by means of a decomposition of heads in the manner shown by Anochikwa et al. (2012) (see Supplement).

### 3.4 The influence of pumping

Introduction of pumping from the depth interval 50–100 m causes hydraulic disequilibrium which continues well beyond the 10 years of simulation, as the head drawdown propagates deep into the profile. As well as drawing water from storage at depth, pumping induces recharge from the surface, there being a downward hydraulic gradient from the surface to the pumped horizon, and upwards from the deeper levels to the pumped horizon. Variable perturbation due to the “IN” surface load is nevertheless clearly evident in the deep groundwater head measurements following correction for secular decline (Fig. 4e). Elastic displacement, manifested as ground surface decline, exceeds 40 cm after 10 years of pumping but, as in the un-pumped “IN” scenario, the annual fluctuation due to surface loading is vanishingly small (0.03 mm). Thus, in addition to the possibility of irreversible plastic deformation, elastic strain may gradually increase due to continuous pumping as stored water is drawn from increasing depths.

Intermittent pumping strongly increases the seasonal variation in heads at the depth of pumping, and this disturbance diffuses to adjacent levels. However, as in the case of continuous pumping, the surface load signal is largely preserved in the deep groundwater head response at 300 m. Also, intermittent pumping induces the same average long-term secular decline in stored water volume and ground surface dis-

placement as continuous pumping, but with additional annual fluctuation caused by the pump switching on and off (decline/drawdown during the dry period when the pumps are used for irrigation and recovery during the rainy season when the pumps are off).

### 3.5 Model results for ground surface displacement

Taking into account a small correction for the compressibility of water, surface displacement in the model is almost equal to the total change in elastic storage in the permanently saturated aquifer. For the cases where pumping dominates the removal of water, surface displacement is in phase with the pumping (Fig. 4f). For the cases which set up a diffusion of the hydraulic signal between the surface boundary and the aquifer, the phase of surface displacement depends on the hydraulic (non-loading) head changes at all depths (Fig. 4b, c, d). Therefore the lag for vertical displacements under the “LD” surface condition is  $\sim \pi$  out of phase with displacement under the “WT” condition. Note from Eq. (6) that the amplitude and lag are both a function of  $\theta = z\sqrt{\frac{\omega}{2D}} = z\sqrt{\frac{\pi}{DT}}$ , and therefore the solutions given here would be scaled in  $z$  by any changes to bulk diffusivity,  $D$ , and signal frequency (or time period,  $T$ ): higher frequency would give the same distribution but for a smaller  $z$ , and the reverse would be true for diffusivity. Intermittent pumping produces the largest cyclic displacements, however, of the order of centimetres, because this condition causes the greatest volume of seasonal drainage from the formation itself. Where there is non-uniform loading, as produced for example by a variable river stage, lateral groundwater drainage may occur and surface vertical displacements may be greater under these conditions too.

## 4 Applying the partial-coupling analysis to field data

Applying the 1-D partial-coupling analysis to field data, we examine poro-mechanical perturbations at two sites, Khulna and Laksmipur in southern Bangladesh (Fig. 1). Hourly measurements of groundwater pressure made between April 2013 and June 2014 in three closely spaced piezometers between 60 and 275 m depth at each site are illustrated as hydrographs of equivalent freshwater head in the Supplement. Data on changes of the actual water table at the field sites are unfortunately not available.

The objective here is to apply the principles and assumptions of the partially coupled hydro-mechanical approach to reproduce the characteristic features of the multi-level groundwater hydrographs using broadly representative aquifer parameters, rather than to attempt an exact match by inverse modelling. Inspection of the hydrographs at both sites indicates, by reference to Figs. 4 and 5, that mechanical loading significantly influences the measured heads. Additionally, the presence of thick clay aquitards at both sites (Figs. 6,

7) suggests conditions under which heads may be determined solely by mechanical loads and piezometers might behave as geological weighing lysimeters, a possibility which we put to the test.

The approach at each site is as follows.

- i. A two-component sand–clay stratigraphy is based on site data, and parameter values are selected from the ranges described in Sect. 2.
- ii. The piezometric readings are compared to examine possible pumping influences which need to be taken into account in the model by means of a simple abstraction pattern. Based on what is known about nearby abstractions an appropriate pumping depth interval is determined. The magnitude of the extraction rate is manually adjusted as a fitting parameter.
- iii. Where a piezometer is uninfluenced by pumping, we test its behaviour as a geological weighing lysimeter. The heads in the chosen piezometer are assumed to define the mechanical load at the surface, and this assumption is tested for self-consistency by comparison of the simulations to the data from all three piezometers.
- iv. The nature of the upper head boundary is then examined by reference to the implications for a variety of hydraulic loading conditions. For a “WT” boundary, changing  $S_y$  manually as a fitting parameter adjusts the magnitude of the applied heads concomitant with the mechanical load.

### 4.1 Groundwater levels at Khulna, south-western Bangladesh

At Khulna (Burgess et al., 2014), piezometers KhPZ60, KhPZ164, and KhP271 (the numbers indicate depth to the piezometer screen in metres) are located 700 m from the  $\sim 300$  m wide tidal Rupsa River, in a grassy compound which also contains municipal water-supply pumping boreholes (Supplement). The lithological sequence (Fig. 6) comprises a surface clay layer overlying sand in which KhPZ60 is screened and a deeper layer of clay at 100 m separating the shallow sand from a deeper sand formation in which KhPZ164 and KhPZ271 are screened. Year-round pumping from 250 to 300 m depth maintains a consistent downward head difference of  $\sim 3$  m between the uppermost and the lower two piezometers. It is the transient head variations rather than the absolute steady-state head differences that are of interest here. Bodies of standing water in the vicinity, water in the unsaturated zone, and shallow groundwater combine with the sinuous Rupsa River as sources of TWS load; groundwater pumping is an additional source of hydraulic variation.

The three Khulna hydrographs are characterized by periodic variations containing tidal frequency components throughout the rising and falling limb of the annual cycle,

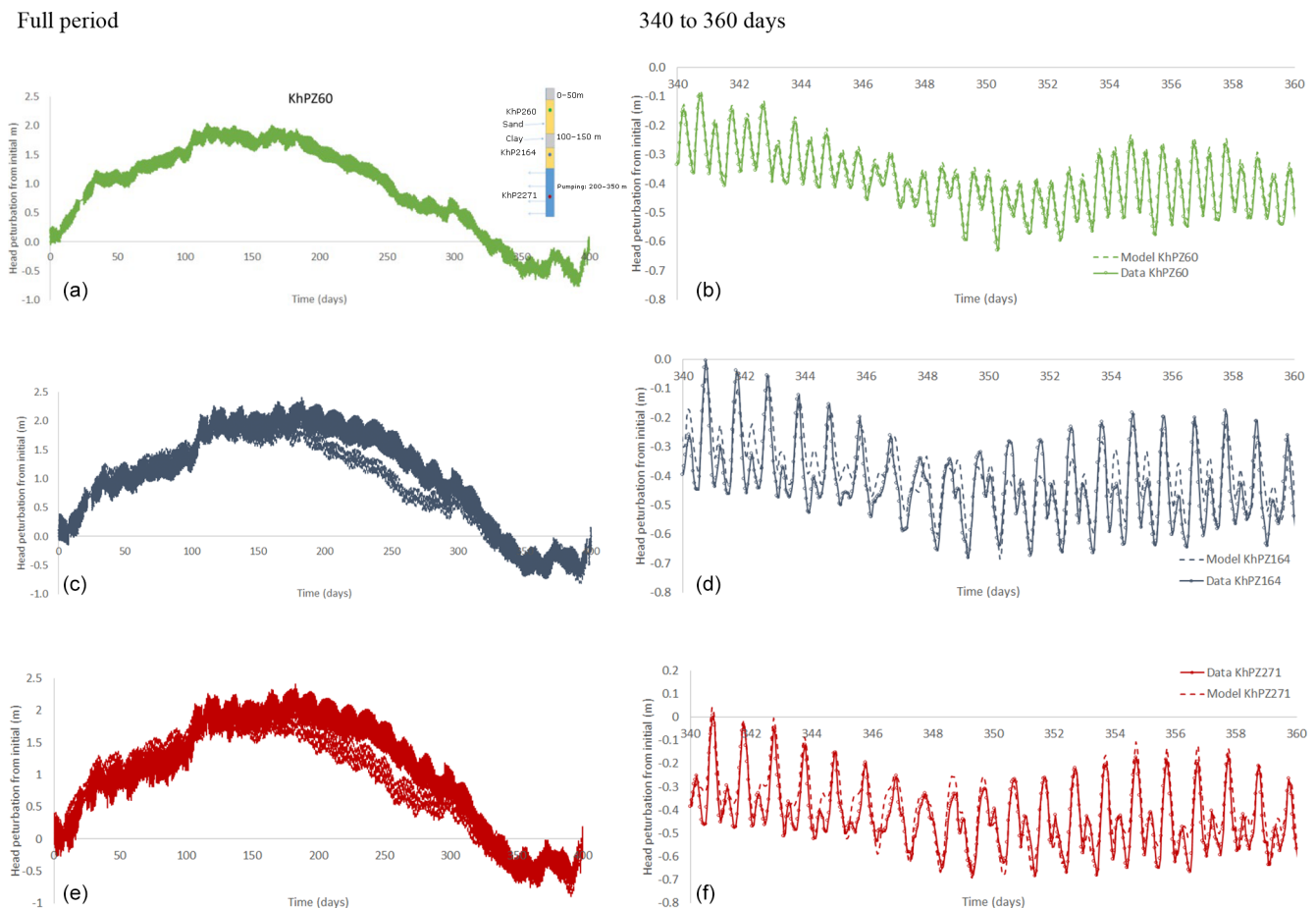


**Figure 6.** Khulna: comparison of observed heads (solid lines) and simulated heads (dashed lines), starting 27 April 2013, for the WT upper boundary condition ( $S_y = 0.4$ ). The  $x$  axis is time in days. The surface loading is set equal to the observed head in KhPZ60, and the surface head is set to the observed head in KhPZ60 divided by  $S_y$ . The pumping rate is  $2.4 \text{ m a}^{-1}$  for 12 h of each day, switching on at 05:45 (Bangladesh Standard Time). Panels (a, b) are KhPZ60 (green), panels (c, d) are KhPZ164 (blue), and panels (e, f) are KhPZ271 (red).

and a series of episodic increments superimposed on the rising limb during the monsoon season; the annual amplitude of groundwater head variation is  $\sim 2.5$  m. The amplitude of the tidal frequency components increases between 60 m and 164 to 271 m depth, with no phase lag and with a consistent synchronicity between the piezometer heads and the Rupsa River water level fluctuations, including the semi-diurnal and spring-neap cycles (Fig. 6 and Supplement). Episodic deflections on the hydrograph rising limbs, coincident with rainfall events, are likewise simultaneous at all measurement depths (Burgess et al., 2014). Therefore, by reference to the partial coupling analysis (Figs. 4 and 5), it is evident that heads in the Khulna piezometers respond primarily to mechanical loading by a combination of monsoon water and tidal loading.

At a daily level the time series of groundwater heads in KhPZ164 and KhPZ271 include an additional frequency component which simple analysis of head differences confirms as the hydraulic influence of the daily municipal pump-

ing schedule from which KhPZ60 is protected by an intermediate clay layer. Therefore KhPZ60 alone is taken as recording a solely mechanical loading response and the KhPZ60 head record is applied as the upper boundary condition to represent the varying TWS load at the surface in a 1-D hydro-mechanical model of the Khulna site (Fig. 6), assuming  $\xi = 1$ . The upper boundary resolves all sources of load acting at the site, including from the Rupsa River, which is a linear rather than an areally extensive load. The ratio of daily (tidal) variability in head at KhPZ60 and in the Rupsa River level is  $\sim 0.06$ . At an equivalent loading efficiency, the 1.23 m annual variation in river stage would explain  $\sim 0.07$  m head variation in KhPZ60, only 3% of the total. While the response of KhPZ60 to the annual changes of the Rupsa River may be greater than to the tidal changes, depending on the details of aquifer structure and hydraulic connection to the river, 97% of the annual variation in head at the piezometer is taken here as attributable to changes in TWS other than load transmitted from the river, representing areally exten-

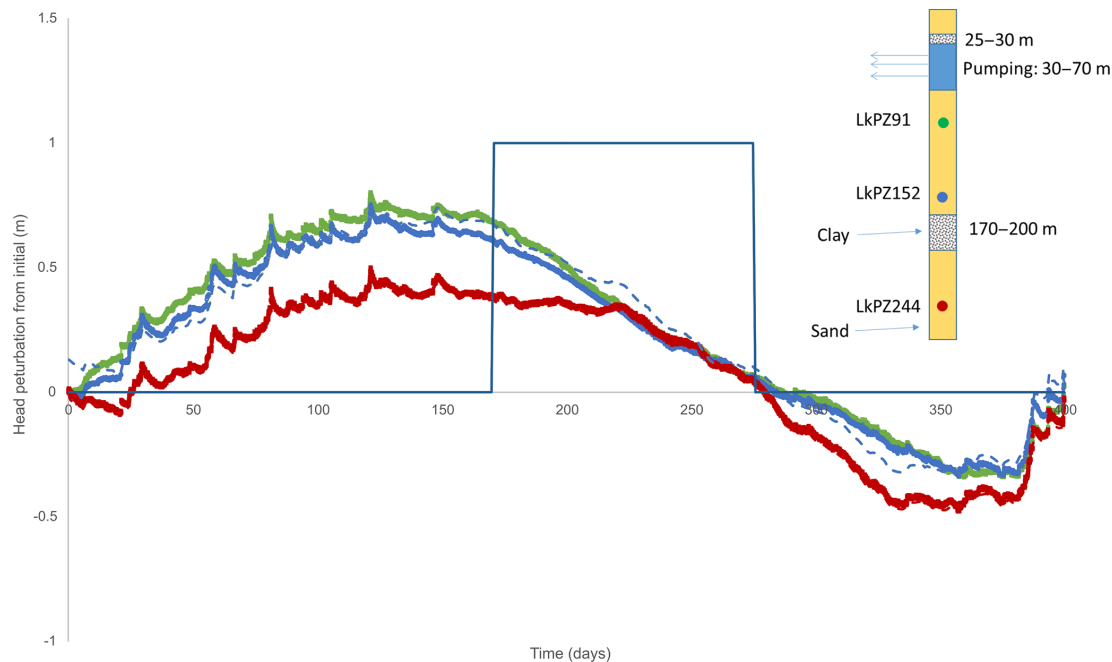


**Figure 7.** Laksmipur: comparison of observed heads (solid lines) and simulated heads (dashed lines) starting 31 May 2013, for the “WT” upper boundary condition ( $S_y = 0.8$ ), and for LkPZ91 (green), LkPZ152 (blue), and LkPZ244 (red). The  $x$  axis is time in days. The surface loading is set equal to the observed head in LkPZ244, and the surface head is set to the observed head in LkPZ244 divided by  $S_y$ . The pumping rate is  $0.04 \text{ m a}^{-1}$  for the period shown (1 for “on”, 0 for “off”).

sive loads as required by the 1-D partially coupled analysis. This is likely an over-estimate; measurements of true water table fluctuation and surface flooding depths in the vicinity are necessary to constrain the hydro-mechanical model more closely. Given the relatively well-drained urban context at Khulna and the absence of areally extensive open water that otherwise characterizes the rural areas of the GBM floodplains, a “WT” condition is most likely the dominant loading style, but other sources of loading may also contribute. The layered structure of the Khulna model (Fig. 6) has clay at 0–50 and 100–150 m with sand in between. The daily municipal pumping cycle is implemented as a source term of  $2.4 \text{ m a}^{-1}$  for 12 h of each day applied over the interval 200 to 350 m, the rate having been manually adjusted by reference to the daily head fluctuations in KhPZ164 and KhPZ271.

Figure 6 compares the measured groundwater heads with the heads simulated by the model under the assumption of a “WT” boundary with  $S_y$  assigned a value of 0.4, with  $\kappa_{\text{sand}} = 1 \times 10^{-5} \text{ m s}^{-1}$ ,  $\kappa_{\text{clay}} = 1 \times 10^{-9} \text{ m s}^{-1}$ ,  $S_s = 10^{-4} \text{ m}^{-1}$  (corresponding to  $E = 82.07 \text{ MPa}$ ),  $\nu = 0.25$ , and  $n = 0.1$ . The results are insensitive to  $S_y$  being varied in the range from 0.1 to 1 (the latter being equivalent to an “IN” boundary), and are near identical in the case of a “LD” boundary (Supplement). This is because the upper clay effectively isolates the piezometers from the surface hydraulically.

#### 4.2 Groundwater levels at Laksmipur, south-eastern Bangladesh

At Laksmipur (Burgess et al., 2017) the piezometers LkPZ91, LkPZ152, and LkPZ244 are situated in a rural region of rice-paddy and tree plantations on the Lower Meghna floodplain (Supplement), 10 km distant from the River Meghna and 8 km from municipal boreholes which pump from 270 to 300 m depth. Seasonal pumping from depths up to 100 m for rice irrigation is common in the vicinity. The lithological sequence indicates fine sand with occasional silty clay layers. The hydrographs are characterized by a sequence of episodic increments in groundwater head associated with periods of heavy rainfall producing a rising limb of amplitude  $\sim 1 \text{ m}$  through the monsoon season; during the dry-season recession, minor periodic fluctuations of order 0.01 m containing atmospheric frequency components become more clearly evident (Burgess et al., 2017). The episodic increments are almost synchronous and of consistent magnitude at all piezometer depths, indicative by reference to Figs. 4 and 5 of groundwater heads responding dominantly to mechanical loading and unloading due to changes in TWS above the aquifer surface.

Here, cyclical head differences between LkPZ244 and the shallower two piezometers indicate hydraulic influences of dry-season pumping on the LkPZ91 and LkPZ152 hydrographs, whereas downward propagation of the hydraulic signals to LkPZ244 is prevented by the clay layer at 170 m

depth. Therefore LkPZ244 is taken as recording a solely mechanical loading response and the LkPZ244 head record is applied as the upper boundary condition to represent the varying TWS load at the surface in a 1-D hydro-mechanical model of the Laksmipur site (Fig. 7), with a small offset applied to the initial heads above 170 m depth, consistent with the observed head perturbations being shown as starting from a common zero value. The stratigraphy as modelled draws from the detail of the drillers' log at Laksmipur (Burgess et al., 2017) and the general form of the stratigraphy as seen across the GBM floodplains (Fig. 2). All styles of upper boundary were applied ("IN", "LD", and "WT" with a range of  $S_y$  values; see the Supplement) in an attempt to distinguish the dominant source of TWS load around the site from the boundary style leading to the best fit with piezometer measurements. In all other respects the models incorporate the dimensions and assumptions as described in Sect. 3, with sand ( $\kappa_{\text{sand}} = 1 \times 10^{-5} \text{ m s}^{-1}$ ) and two clay layers (BWDB, 2013) at 25–30 and 170–200 m ( $\kappa_{\text{clay}} = 1 \times 10^{-8} \text{ m s}^{-1}$ ), and  $E = 82.07 \text{ MPa}$ . A simple dry-season pumping regime over a 105 d period starting 17 November 2013 is implemented as a source term of  $0.04 \text{ m a}^{-1}$  applied over the interval 30 to 70 m in the model, manually adjusted by reference to the LkPZ91 and LkPZ152 hydrographs.

For LkPZ244 the simulated heads are an excellent match with measurements over the entire period. The simulated heads for the shallower two piezometers LkPZ91 and LkPZ152 most closely match the measurements under a "WT" boundary with  $S_y$  assigned a value of 0.8 (Fig. 7 and the Supplement). The model results therefore confirm that LkPZ244 is isolated from the hydraulic effects of water table variation and of seasonal pumping, and the LkPZ244 groundwater head variation over the observation period is determined solely by mechanical loads at the surface. Therefore LkPZ244 is validated as acting effectively as a geological weighing lysimeter (Burgess et al., 2017).

For the shallower piezometers, the best fit value for  $S_y$  is higher than is reasonable for fine sand and more likely indicates the combined effects of a variable water table and fluctuating levels of standing water, in drainage channels, and on paddy fields around the piezometer site, consistent with the field situation. As a consequence of seasonal pumping at  $0.04 \text{ m a}^{-1}$ , the model shows groundwater is both drawn from storage and induced as recharge from the upper surface, but the amplitude of saturated storage fluctuation is only 6 mm; therefore, changes to the water budget are dominated by recharge to the water table. The surface displacement is predicted at 6 mm amplitude, in phase with the changes in storage.

## 5 Discussion

### 5.1 Aquifer responses to discrete modes of terrestrial water variation

Models based on the 1-D partially coupled hydro-mechanical analysis confirm that substantial poroelastic influences should be expected in the Bengal Aquifer System, and that groundwater heads respond characteristically to changes in specific terrestrial water stores (Figs. 4 and 5). Only laterally extensive flooding above an aquifer fully saturated to the ground surface (the "IN" loading style) will drive instantaneous and synchronous head variations at all depths determined by the loading efficiency, inducing negligible flow of groundwater. In any situation involving a variable water table (the "WT" loading style) and for any variable loads hydraulically disconnected from the aquifer (the "LD" style), hydraulic gradients are imposed due to the unequal magnitude of stress and head at the surface. These gradients take time to dissipate, depending on the frequency of the signal fluctuation and the aquifer hydraulic diffusivity, and so lead to differences in amplitude and phase of the head response with depth. In these situations, the relative importance of the hydraulic and mechanical influence is controlled by the aquifer hydraulic diffusivity, the loading efficiency, and the depth of interest. In the case of a fluctuating water table, the difference between the head and stress signals is a function of the specific yield,  $S_y$ , in the zone of fluctuation.

The characteristic responses of the aquifer might therefore provide a key to identifying the terrestrial water store dominating  $\Delta\text{TWS}$ , by monitoring vertical profiles of groundwater head. Multiple terrestrial water stores will normally contribute, however, as at Laksmipur and Khulna, so a unique identification may not be possible. This limitation is inherent to the 1-D analysis, which resolves all the contributions to load into one upper boundary condition respectively for head and stress. The analysis indicates how different loads and dynamic responses superpose to produce the observed groundwater hydrographs. In principle, key aspects of the water balance may be better estimated by de-convolving known components of the  $\Delta\text{TWS}$  signal. Anochikwa et al. (2012) assembled field measurements of rainfall and evapotranspiration at a site in Saskatchewan, Canada, using them to define the upper boundary conditions in a 1-D model to examine their hydraulic and mechanical loading separately, before summing the outcomes to simulate the overall hydro-mechanical influence on groundwater pressure. Having determined loading efficiency by reference to barometric effects, they then calibrated their 1-D model against observed groundwater pressures by varying hydraulic conductivity. At Khulna and Laksmipur, measurements of the separate components of the terrestrial water cycle were not available, and hence an indirect demonstration of hydro-mechanical effects was desirable. The simulated and observed heads are in good agreement, consistent with the local conditions, so confirm-

ing the 1-D partially coupled analysis as a suitable basis for representing the poroelastic behaviour of the BAS.

## 5.2 Significance for groundwater monitoring and geological weighing lysimetry

In terms of the extent to which piezometer water levels indicate recharge and drainage, it is only where there is a rapid hydraulic connection between the piezometer and the water table that the piezometer will be sensitive to head change at the water table and therefore to changes in unconfined storage. If a piezometer is hydraulically isolated from surface water and/or the water table and is beyond other transient hydraulic influences, it can respond to changes in the weight of the TWS load, acting as a geological weighing lysimeter (van der Kamp and Maathuis, 1991; Smith et al., 2017). In this case, where the changing load is due to a moving water table, knowledge of the loading efficiency allows the load measurement to be converted into an estimate of recharge and discharge.

In all other situations, a wide range of coupled hydro-mechanical responses can be expected, as we have shown for the BAS (Figs. 4 and 5). Seasonally variable groundwater heads (Fig. 4) are therefore open to misinterpretation as seasonally variable groundwater storage, leading to error in determination of recharge if the poroelastic nature of the response is neglected. Consider heads at 30 m, a common depth for Bangladesh Water Development Board (BWDB) monitoring boreholes (Shamsudduha et al., 2011). For the case of a variable load hydraulically disconnected from the aquifer (Fig. 4d), the annual water level rise is equal to half the amplitude of the load, yet augmentation of elastic storage, by definition in this case, is nil. For the case of variable TWS inundation (Fig. 4a) the annual groundwater level rise is equivalent to the annual depth of inundation, yet augmentation of elastic and unconfined storage is insignificant. Conversely, relative to a variable water table (Fig. 4b, c), groundwater fluctuation at 30 m depth is attenuated. Failure to account for this would lead to an underestimate of recharge to unconfined storage by about 30 %. The error increases as hydraulic diffusivity decreases; therefore, errors could be expected to be greater in the coastal regions of the Bengal Basin, where the thickness of silty clays is greater (Mukherjee et al., 2007). Considerable caution is therefore necessary in the use of even relatively shallow piezometers as indicators of recharge to the water table. A true indication of recharge requires either a shallow tubewell screened over the depth interval of actual water table fluctuation or a deep piezometer responding as a geological weighing lysimeter to the varying mass provided by a fluctuating water table. In the latter case it is recharge to the shallow water table that is measured, not recharge at the depth of the piezometer.

The 1-D hydro-mechanical framework can be applied as a test for the special cases where groundwater head responds solely to mechanical load, and hence to validate the use of

geological weighing lysimetry. The laterally extensive loading criterion inherent to the 1-D analysis must apply, and the piezometer screen must be isolated or distant from hydraulic transients originating at the surface or from pumping. We have shown for the BAS that these requirements most likely occur at depths beyond about 250 m, as in the case of “WT” and “LD” loading styles in the absence of pumping (Fig. 5). The inundation (“IN”) style of TWS variation leads to instantaneous transmission of head without loss of amplitude at all depths; in this case piezometers at all depths provide a mechanical record of  $\Delta$ TWS rather than a hydraulic record of storage variation, and to infer recharge would lead to 100 % error. Our analysis demonstrates a solely mechanical loading response at 244 m depth at Laksmipur, below the level of seasonal irrigation pumping, and at 60 m depth at Khulna, above the level of deep pumping for municipal water supply.

## 5.3 Significance for ground surface displacements and groundwater storage changes

The models also demonstrate the amplitude and phase of ground surface displacement as a hydro-mechanical consequence of varying terrestrial water stores, and the significance of pumping (Fig. 4e and f). Under simplifications associated with the 1-D model, vertical surface displacements relative to a fixed model base at 1 km depth are approximately equal to the change in elastic storage, the small difference being due to compressibility of water. These changes are minor in the BAS under all TWS loading styles, of the order of millimetres, compared to the displacements in the case of seasonal groundwater pumping, which are of the order of centimetres. Seasonal surface displacements of the order of centimetres have also been attributed to strain acting over a depth scale of hundreds of kilometres due to the load applied by monsoonal inundation over the entire Bengal Basin (Steckler et al., 2010). Strains due to seasonal groundwater pumping at shallow depths may therefore be of the same order of magnitude but out of phase with crustal strain, making ground surface deflections a poor proxy for changing elastic storage in the aquifer. As a corollary, interpretation of seasonal ground surface fluctuations across the GBM floodplains solely in terms of deep crustal deformation (Steckler et al., 2010) potentially requires reassessment in the light of BAS aquifer poroelasticity.

## 5.4 Limitations and further consequences

In our analysis we have based values for the 1-D loading efficiency,  $\xi$  (0.932–0.993), and Young’s modulus,  $E$  (82–851 MPa), in the BAS on field measurements of  $S_s$ , for the sake of internal hydro-mechanical consistency, but we have noted a discrepancy with lower values for the 1-D loading efficiency  $\xi$  (0.69–0.87) derived from determinations of barometric efficiency (Burgess et al., 2017). These differences require attention, but the overall conclusions on the signif-

icance of poroelastic behaviour in the BAS and the pattern of poroelastic responses characteristic of specific upper surface TWS boundary conditions are unaffected. Although we omitted barometric effects in the generic simulations for the sake of simplicity, it is straightforward to superpose a further loading signal on top of the existing one if required, as for example when deconvolving deep piezometric signals to make water resources assessments (Anochikwa et al., 2012).

Data on changes in the water table would have greatly helped the analysis of loading effects at Khulna and Laksmipur. It is strongly recommended that in future hydro-mechanical analyses of the groundwater dynamics of large layered aquifers such as the BAS, both water table data and deeper head data should be obtained. For the water table, this requires a shallow piezometer to be screened across the full range of fluctuation of the true water table.

Under certain circumstances the extensive load assumption inherent in the 1-D analysis may break down. Rivers, as linear sources of head and load, can be accommodated within the 1-D framework where their contribution to the TWS load is minor as demonstrated at Khulna. In general, however, rivers should be expected to impose laterally variable heads and require a more generalized 2-D or 3-D fully coupled poro-mechanical treatment (Boutt, 2010; Pacheco and Fallico, 2015). An equivalent constraint applies to strains, an additional reason for surface displacement not to offer a secure proxy for groundwater storage in the BAS. The dense distribution of rivers, distributaries, and drainage channels in the Bengal Basin makes the BAS widely vulnerable to loading effects that may not adequately be reduced to a 1-D description; 13 % and 47 % of 1035 piezometers in the BWDB groundwater monitoring network lie within 1 and 5 km respectively of a river.

## 6 Conclusions

We argue that a 1-D *partially coupled* approach to hydro-mechanical processes, whereby the loading term is included in the flow equation without the need to simultaneously compute the elastic equation, is a suitable basis for representing the poroelastic behaviour of the Bengal Aquifer System when surface conditions can be treated as areally extensive. Applying a 1-D *partially coupled* hydro-mechanical analysis, we have shown how the BAS responds characteristically to specific sources of terrestrial water storage variation. Rivers can be incorporated as a component of the 1-D load where their contribution is small, but in general will require a 2-D or fully 3-D treatment.

Groundwater levels, groundwater recharge, vertical groundwater flow, and ground surface elevations are all influenced by the poroelastic behaviour of the BAS. Our results expose the error of the conventional assumption of decoupled hydraulic behaviour which underlies previous assessments of recharge to the BAS. Also, they demonstrate the complexities in applying ground surface displacements as a proxy measure for variations in groundwater storage. We propose that the 1-D *partially coupled* analysis can be applied to validate when geological weighing lysimetry is applicable in the BAS. In some situations, geological weighing lysimetry offers an alternative approach to recharge assessment.

*Data availability.* The datasets analysed during the current study are available from the corresponding author on request.

### Appendix A: Poro-mechanical equations

The constitutive isotropic relation between elastic stress and strain, coupled to the pore pressure by Terzaghi's effective stress law, is given by (Neuzil, 2003)

$$\sigma_{ij} = 2G\varepsilon_{ij}\delta_{ij} + 2G\frac{\nu}{1-2\nu}\varepsilon_{kk}\delta_{ij} + \alpha_B p\delta_{ij}, \quad (\text{A1})$$

where  $\delta_{ij}$  is the Kronecker delta (which is zero when  $i \neq j$  and one when  $i = j$ ) and follows the Einstein summation convention; stresses ( $\sigma_{ij}$ ) and strains ( $\varepsilon_{ij}$ ) are positive in compression;  $p$  is the porewater pressure (Pa),  $\nu$  is Poisson's ratio (-),  $G$  is the shear modulus (MPa), and  $\alpha_B = 1 - K/K_s$ , where  $K$  (MPa) is the bulk modulus of the porous medium and  $K_s$  (MPa) is the bulk modulus of the solid grains.

Just as the elastic equations have a pore pressure term, the isothermal, Darcian groundwater flow equation contains a coupled stress term (Neuzil, 2003):

$$\nabla \cdot \kappa (\nabla p + \rho g \nabla z) = S_{s3} \frac{\partial p}{\partial t} - S_{s3} \beta \frac{\partial \sigma_t}{\partial t} - gJ, \quad (\text{A2})$$

where  $\kappa$  is the hydraulic conductivity ( $\text{m s}^{-1}$ ),  $p$  is the pore pressure (Pa),  $z$  is the elevation (m),  $J$  is a source term used here to simulate groundwater abstraction by pumping, and  $\sigma_t = (\sigma_{xx} + \sigma_{yy} + \sigma_{zz})/3$  (Pa).

The 3-D specific storage is defined as

$$S_{s3} = \rho g \left[ \left( \frac{1}{K} - \frac{1}{K_s} \right) + \left( \frac{n}{K_f} - \frac{n}{K_s} \right) \right], \quad (\text{A3})$$

where  $n$  is the porosity and  $K_f$  is the modulus of the water (MPa).

The (3-D) loading efficiency, or Skempton's coefficient,  $\beta$ , is defined as

$$\beta = \frac{\left( \frac{1}{K} - \frac{1}{K_s} \right)}{\left( \frac{1}{K} - \frac{1}{K_s} \right) + \left( \frac{n}{K_f} - \frac{n}{K_s} \right)}. \quad (\text{A4})$$

Where there is areally extensive loading, the 1-D loading efficiency is given by

$$\xi = \beta(1 + \nu) / [3(1 - \nu) - 2\alpha_B\beta(1 - 2\nu)]. \quad (\text{A5})$$

The 1-D specific storage is given by

$$S_s = S_{s3}(1 - \lambda\beta), \quad (\text{A6})$$

where  $\lambda = 2\alpha_B(1 - 2\nu)/3(1 - \nu)$ .

### Appendix B: Nomenclature

$\alpha$	Proportion of mechanical load as head
$\alpha_B$	Biot–Willis coefficient, $1 - K/K_s$
$\beta, C$	3-D loading efficiency, Skempton's coefficient, or "tidal efficiency"
$\delta_{ij}$	Kronecker delta
$\varepsilon_{ij}$	Strain
$\theta$	$z\sqrt{\frac{\omega}{2D}} = z\sqrt{\frac{\pi}{DT}}$
$\lambda$	$2\alpha_B(1 - 2\nu)/3(1 - \nu)$
$\nu$	Poisson's ratio
$\xi$	1-D loading efficiency
$\kappa$	Hydraulic conductivity
$\rho$	Water density
$\sigma_{ij}$	Stress tensor
$\sigma_t$	Total stress
$\psi$	Lag (radians)
$\omega$	Angular frequency
$a$	River half-width
$B$	Barometric efficiency
$E$	Young's modulus
$D$	Hydraulic diffusivity
$g$	Acceleration due to gravity
$G$	Shear modulus
$h$	Head
$H(t)$	Top boundary head
$H_0$	Amplitude of top boundary head
$J$	Fluid source term
$K$	Bulk modulus of porous medium
$K_f$	Bulk modulus of the water
$K_s$	Bulk modulus of the solid grains
$L(t)$	Top boundary load
$L_0$	Amplitude of top boundary load
$n$	Porosity
$p$	Pore pressure
$S_y$	Specific yield
$S_s$	Specific storage
$S_{s3}$	3-D specific storage
$t$	Time
$u$	Vertical displacement
$x$	Perpendicular distance from a river
$z$	Vertical coordinate



*Supplement.* The supplement related to this article is available online at: <https://doi.org/10.5194/hess-23-2461-2019-supplement>.

*Author contributions.* WGB conceived the study; NDW led the modelling; all the authors contributed to the scenario descriptions and consideration of the modelling results; NDW and WGB drafted the manuscript; all the authors reviewed the manuscript.

*Competing interests.* The authors declare that they have no conflict of interest.

*Acknowledgements.* We acknowledge funding from the UK EPSRC Global Challenges Research Fund (UCL/BEAMS EPSRC GCRF award 172313, EP/P510890/1) to William G. Burgess for research on *Poroelasticity in the Bengal Aquifer System and groundwater resources monitoring in Bangladesh*. Nicholas D. Woodman thanks the University of Southampton for leave of absence during the course of the project. Field measurements at Khulna and Laksmipur were made with the kind assistance of the Bangladesh Water Development Board (BWDB) and financial support from the UK Department for International Development (DfID) under the project *Groundwater Resources in the Indo-Gangetic Basin* (Grant 202125-108) managed by Alan MacDonald of the British Geological Survey. We are grateful to Mike Steckler, Columbia University, and Humayun Akhter, Dhaka University, for useful discussions on ground surface vertical motions in the Bengal Basin, and to John Barker and William Powrie for helpful discussion of the fundamental processes at the start of the research. Mohammed Shamsudduha, University College London, and Sarmin Sultana, Dhaka University, are thanked for discussions on the hydrological context of the groundwater level monitoring piezometers. We thank one anonymous reviewer whose comments and advice helped improve the manuscript.

*Review statement.* This paper was edited by Monica Riva and reviewed by two anonymous referees.

## References

- Acworth, R. I., Rau, G. C., McCallum, A. M., Andersen, M. S., and Cuthbert, M. O.: Understanding connected surface-water/groundwater systems using Fourier analysis of daily and sub-daily head fluctuations, *Hydrogeol. J.*, 23, 143–159, <https://doi.org/10.1007/s10040-014-1182-5>, 2015.
- Anochikwa, C. I., van der Kamp, G., and Barbour, S. L.: Interpreting pore-water pressure changes induced by water table fluctuations and mechanical loading due to soil moisture changes, *Can. Geotech. J.*, 49, 357–366, 2012.
- Bakker, M.: The effect of loading efficiency on the groundwater response to water level changes in shallow lakes and streams, *Water Resour. Res.*, 52, 1075–1715, <https://doi.org/10.1002/2015WR017977>, 2016.
- Bardsley, W. E. and Campbell, D. J.: A new method for measuring near-surface moisture budgets in hydrological systems, *J. Hydrol.*, 154, 245–254, 1994.
- Bardsley, W. E. and Campbell, D. J.: Natural geological weighing lysimeters: calibration tools for satellite and ground surface gravity monitoring of subsurface water-mass change, *Natural Resources Research*, 9, 147–156, 2000.
- Bardsley, W. E. and Campbell, D. J.: An expression for land surface water storage monitoring using a two-formation geological weighing lysimeter, *J. Hydrol.*, 335, 240–246, 2007.
- Barr, A. G., van der Kamp, G., Schmidt, R., and Black, T. A.: Monitoring the moisture balance of a boreal aspen forest using a deep groundwater piezometer, *Agr. Forest Meteorol.*, 102, 13–24, 2000.
- Benner, S. G., Polizzotto, M. L., Kocar, B. D., Ganguly, S., Phan, K., Ouch, K., Sampson, M., and Fendorf, S.: Groundwater flow in an arsenic-contaminated aquifer, Mekong Delta, Cambodia, *Appl. Geochem.*, 23, 3072–3087, 2008.
- Bense, V. F. and Person, M. A.: Transient hydrodynamics within intracratonic sedimentary basins during glacial cycles, *J. Geophys. Res.-Earth*, 113, F04005, <https://doi.org/10.1029/2007JF000969>, 2008.
- Black, J. H. and Barker, J. A.: The puzzle of high heads beneath the West Cumbrian coast, UK: a possible solution, *Hydrogeol. J.*, 24, 439–457, <https://doi.org/10.1007/s10040-015-1340-4> 2016.
- Boutt, D. F.: Poroelastic loading of an aquifer due to upstream dam releases, *Ground Water*, 48, 580–592, 2010.
- Burbey, T. J., Warner, S. M., Blewitt, G., Bell, J. W., and Hill, E.: Three-dimensional deformation and strain induced by municipal pumping, part 1: Analysis of field data, *J. Hydrol.*, 319, 123–142, 2006.
- Burgess, W. G., Hoque, M. A., Michael, H. A., Voss, C. I., Breit, G. N., and Ahmed, K. M.: Vulnerability of deep groundwater in the Bengal Aquifer System to contamination by arsenic, *Nat. Geosci.*, 3, 83–87, <https://doi.org/10.1038/ngeo750>, 2010.
- Burgess, W. G., Shamsudduha, M., Taylor, R. G., Zahid, A., Ahmed, K. M., Mukherjee, A., and Lapworth, D. J.: Seasonal, episodic and periodic changes in terrestrial water storage recorded by deep piezometric monitoring in the Ganges/Brahmaputra/Meghna delta, AGU Fall Meeting 2014, 15–19 December 2014, San Francisco, USA, 2014.
- Burgess, W. G., Shamsudduha, M., Taylor, R. G., Zahid, A., Ahmed, K. M., Mukherjee, A., Lapworth, D. J., and Bense, V. F.: Terrestrial water load and groundwater fluctuation in the Bengal Basin, *Sci. Rep.*, 7, 3872, <https://doi.org/10.1038/s41598-017-04159-w>, 2017.
- BWDB (Bangladesh Water Development Board): Establishment of monitoring network and mathematical model study to assess salinity intrusion in groundwater in the coastal area of Bangladesh due to climate change, Final report, Dhaka, Bangladesh, 1678 pp., 2013.
- Chaussard, E., Burgmann, R., Shirzaei, M., Fielding, E. J., and Baker, B.: Predictability of hydraulic head changes and characterization of aquifer-system and fault properties from InSAR-derived ground deformation, *J. Geophys. Res.-Sol. Ea.*, 119, 6572–6590, <https://doi.org/10.1002/2014JB011266>, 2014.
- COMSOL Multiphysics®: COMSOL AB, Stockholm, Sweden, v. 5.2., <https://www.comsol.com/>, last access: 27 November 2018.

- de Silva, S., Wightman, N. R., and Kamruzzaman, M.: Geotechnical ground investigation for the Padma Main Bridge, IABSE-JSCE Joint Conference on Advances in Bridge Engineering-II, 8–10 August 2010, Dhaka, Bangladesh, 2010.
- Domenico, P. A. and Schwartz, F. W.: *Physical and Chemical Hydrogeology*, 2nd edn., John Wiley & Sons, New York, USA, 1998.
- Erban, L. E., Gorelick, S. M., and Zebker, H. A.: Groundwater extraction, land subsidence, and sea-level rise in the Mekong Delta, Vietnam, *Environ. Res. Lett.*, 9, 084010, <https://doi.org/10.1088/1748-9326/9/8/084010>, 2014.
- Fendorf, S., Michael, H. A., and van Geen, A.: Spatial and temporal variations of groundwater arsenic in south and southeast Asia, *Science*, 328, 1123–1127, 2010.
- Gibson, R. E.: The analytical method in soil mechanics, *Geotechnique*, 24, 115–140, 1974.
- Green, D. H. and Wang, H. F.: Specific storage and poroelastic coefficient, *Water Resour. Res.*, 26, 1631–1637, 1990.
- Hasanuzzaman, S. M.: Impact of groundwater utilisation on agriculture, in: *Groundwater resources and development in Bangladesh: background to the arsenic crisis, agricultural development and the environment*, edited by: Rahman, A. A. and Ravenscroft, P., Bangladesh Centre for Advanced Studies, University Press Ltd., Dhaka, Bangladesh, 161–185, 2003.
- Hoque, M. A., Burgess, W. G., and Ahmed, K. M.: Integration of aquifer geology, groundwater flow and arsenic distribution in deltaic aquifers – A unifying concept, *Hydrol. Process.*, 31, 2095–2109, <https://doi.org/10.1002/hyp.11181>, 2017.
- Hussain, M. M. and Abdullah, S. K. M.: Geological setting of the areas of arsenic safe aquifers. Report of the ground water task force, Ministry of Local Government, Rural Development & Cooperatives, Local Government Division, Bangladesh, Interim Report No. 1, 2001.
- Jacob, C. E.: On the flow of water in an elastic artesian aquifer, *Transactions of the American Geophysical Union*, 574–586, <https://doi.org/10.1029/TR021i002p00574>, 1940.
- Lambert, A., Huang, J., van der Kamp, G., Henton, J., Mazzotti, S., James, T. S., Courtier, N., and Barr, A. G.: Measuring water accumulation rates using GRACE data in areas experiencing glacial-isostatic adjustment: The Nelson River basin, *Geophys. Res. Lett.*, 40, 6118–6122, <https://doi.org/10.1002/2013GL057973>, 2013.
- Larsen, F., Pham, N. Q., Dang, N. D., Postma, D., Jessen, S., Pham, V. H., Nguyen, T. B., Trieu, H. D., Tran, L. T., Nguyen, H., Chambon, J., Nguyen, H. V., Ha, D. H., Hue, N. T., Duc, M. T., and Refsgaard, J. C.: Controlling geological and hydrogeological processes in an arsenic contaminated aquifer on the Red River flood plain, Vietnam, *Appl. Geochem.*, 23, 3099–3115, 2008.
- Manga, M. I., Beresnev, I., Brodsky, E. E., Elkhoury, J. E., Elsworth, D., Ingebritsen, S. E., Mays, D. C., and Wang, C.-Y.: Changes in permeability caused by transient stresses: field observations, experiments, and mechanisms, *Rev. Geophys.*, 50, RG2004, <https://doi.org/10.1029/2011RG000382>, 2012.
- Marin, S., van der Kamp, G., Pietroniro, A., Davison, B., and Toth, B.: Use of geological weighing lysimeters to calibrate a distributed hydrological model for the simulation of land-atmosphere moisture exchange, *J. Hydrol.*, 383, 179–185, 2010.
- Michael, H. A. and Voss, C. I.: Evaluation of the sustainability of deep groundwater as an arsenic-safe resource in the Bengal Basin, *P. Natl. Acad. Sci.*, 105, 8531–8536, 2008.
- Michael, H. A. and Voss, C. I.: Estimation of regional-scale groundwater flow properties in the Bengal Basin of India and Bangladesh, *Hydrogeol. J.*, 17, 1329–1346, <https://doi.org/10.1007/s10040-009-0443-1>, 2009a.
- Michael, H. A. and Voss, C. I.: Controls on groundwater flow in the Bengal Basin of India and Bangladesh: regional modeling analysis, *Hydrogeol. J.*, 17, 1561–1577, <https://doi.org/10.1007/s10040-008-0429-4>, 2009b.
- Mukherjee, A., Fryar, A. E., and Rowe, H. D.: Regional hydrostratigraphy and groundwater flow modeling of the arsenic affected western Bengal basin, West Bengal, India, *Hydrogeol. J.*, 15, 1397–1418, <https://doi.org/10.1007/s10040-007-0208-7>, 2007.
- Narasimhan, T. N.: On storage coefficient and vertical strain, *Ground Water*, 44, 488–491, 2006.
- Neuzil, C. E.: Hydromechanical coupling in geological processes, *Hydrogeol. J.*, 11, 41–83, 2003.
- Pacheco, F. A. L. and Fallico, C.: Hydraulic head response of a confined aquifer influenced by river stage fluctuations and mechanical loading, *J. Hydrol.*, 531, 716–727, <https://doi.org/10.1016/j.jhydrol.2015.10.055>, 2015.
- Powrie, W.: *Soil Mechanics: Concepts and Applications*, 3rd ed., CRC Press, Taylor and Francis Group, Boca Raton, Florida, USA, 2014.
- Rahman, M. A. T., Majumder, R. K., Rahman, S. H., and Halim, M. A.: Sources of deep groundwater salinity in the southwestern zone of Bangladesh, *Environ. Earth Sci.*, 63, 363–373, 2011.
- Ravenscroft, P.: Overview of the hydrogeology of Bangladesh, in: *Groundwater resources and development in Bangladesh: background to the arsenic crisis, agricultural potential and the environment*, edited by: Rahman, A. A. and Ravenscroft, P., Bangladesh Centre for Advanced Studies, University Press Ltd., Dhaka, Bangladesh, 43–86, 2003.
- Ravenscroft, P., Burgess, W. G., Ahmed, K. M., Burren, M., and Perrin, J.: Arsenic in groundwater of the Bengal Basin, Bangladesh: Distribution, field relations, and hydrogeological setting, *Hydrogeol. J.*, 13, 727–751, <https://doi.org/10.1007/s10040-003-0314-0>, 2005.
- Ravenscroft, P., Brammer, H., and Richards, K. S.: *Arsenic pollution: a global synthesis*, First ed., Wiley-Blackwell, UK, 616 pp., 2009.
- Ravenscroft, P., McArthur, J. M., and Hoque, M. A.: Stable groundwater quality in deep aquifers of Southern Bangladesh: The case against sustainable abstraction, *Sci. Total Environ.*, 454–455, 627–638, 2013.
- Reeves, J. A., Knight, R., Zebker, H. A., Kitanidis, P. K., and Schreuder, W. A.: Estimating temporal changes in hydraulic head using InSAR data in the San Luis Valley, Colorado, *Water Resour. Res.*, 50, 4459–4473, <https://doi.org/10.1002/2013WR014938>, 2014.
- Roeloffs, E. A.: Fault stability changes induced beneath a reservoir with cyclic variations in water level, *J. Geophys. Res.*, 93, 2107–2124, 1988.
- Rojstaczer, S. and Agnew, D. C.: The influence of formation material properties on the response of water levels in wells to Earth

- tides and atmospheric loading, *J. Geophys. Res.*, 94, 12403–12411, 1989.
- Shamsudduha, M., Taylor, R. G., Ahmed, K. M., and Zahid, A.: The impact of intensive groundwater abstraction on recharge to a shallow regional aquifer system: evidence from Bangladesh, *Hydrogeol. J.*, 19, 901–916, <https://doi.org/10.1007/s10040-011-0723-4>, 2011.
- Shamsudduha, M., Taylor, R. G., and Longuevergne, L.: Monitoring groundwater storage changes in the highly seasonal humid tropics: validation of GRACE measurements in the Bengal Basin, *Water Resour. Res.*, 48, W02508, <https://doi.org/10.1029/2011WR010993>, 2012.
- Shamsudduha, M., Zahid, A., and Burgess, W. G.: Security of deep groundwater against arsenic contamination in the Bengal Aquifer System: a numerical modelling study in southeast Bangladesh, *Sustainable Water Resources Management*, <https://doi.org/10.1007/s40899-018-0275-z>, 2018.
- Smith, C. D., van der Kamp, G., Arnold, L., and Schmidt, R.: Measuring precipitation with a geolysimeter, *Hydrol. Earth Syst. Sci.*, 21, 5263–5272, <https://doi.org/10.5194/hess-21-5263-2017>, 2017.
- Spane, F. A.: Considering barometric pressure in groundwater flow investigations, *Water Resour. Res.*, 38, 1078, <https://doi.org/10.1029/2001WR000701>, 2002.
- Steckler, M. S., Nooner, S. L., Akhter, S. H., Chowdhury, S. K., Bettadpur, S., Seiber, L., and Kogan, M. G.: Modeling earth deformation from monsoonal flooding in Bangladesh using hydrographic, GPS and GRACE Data, *J. Geophys. Res.*, 115, B08407, <https://doi.org/10.1029/2009JB007018>, 2010.
- Sultana, S., Ahmed, K. M., Mahtab-Ul-Alam, S. M., Hasan, M., Tuinhof, A., Ghosh, S. K., Rahman, M. S., Ravenscroft, P., and Zheng, Y.: Low-cost aquifer storage and recovery: implications for improving drinking water access for rural communities in coastal Bangladesh, *J. Hydrol. Eng.*, 20, B08407, [https://doi.org/10.1061/\(ASCE\)HE.1943-5584.0001100](https://doi.org/10.1061/(ASCE)HE.1943-5584.0001100), 2015.
- Sutherland, R., Townend, J., Toy, V., et al.: Extreme hydrothermal conditions at an active plate-bounding fault, *Nature*, 546, 137–140, <https://doi.org/10.1038/nature22355>, 2017.
- Tam, V. T., Batelaan, O. L. T. T., and Nhan, P. Q.: Three-dimensional hydrostratigraphical modelling to support evaluation of recharge and saltwater intrusion in a coastal groundwater system in Vietnam, *Hydrogeol. J.*, 22, 1749–1762, 2014.
- Tapley, B. D., Bettadpur, S., Ries, J. C., Thompson, P. F., and Watkins, M. M.: GRACE measurements of mass variability in the Earth system, *Science*, 305, 503–505, 2004.
- Tiwari, V. M., Wahr, J., and Swenson, S.: Dwindling groundwater resources in northern India, from satellite gravity observations, *Geophys. Res. Lett.*, 36, L18401, <https://doi.org/10.1029/2009GL039401>, 2009.
- van der Kamp, G. and Gale, J. E.: Theory of Earth tide and barometric effects in porous formations with compressible grains, *Water Resour. Res.*, 19, 538–544, 1983.
- van der Kamp, G. and Maathuis, H.: Annual fluctuations of groundwater levels as a result of loading by surface moisture, *J. Hydrol.*, 127, 137–152, 1991.
- van der Kamp, G. and Schmidt, R.: Monitoring of total soil moisture on a scale of hectares using groundwater piezometers, *Geophys. Res. Lett.*, 24, 719–722, 1997.
- van der Kamp, G. and Schmidt, R.: Review: Moisture loading - the hidden information in groundwater observation well records, *Hydrogeol. J.*, 25, 2225–2233, <https://doi.org/10.1007/s10040-017-1631-z>, 2017.
- Verruijt, A.: Elastic storage of aquifers, in: *Flow through porous media*, edited by: Weist, R. J. M. d., Academic Press Inc., New York, USA, 331–376, 1969.
- Xu, X., Huang, G., Qu, Z., and Pereira, L. S.: Using MODFLOW and GIS to assess changes in groundwater dynamics in response to water saving measures in irrigation districts of the Upper Yellow River Basin, *Water Resources Management*, 25, 2035–2059, 2011.